Catalysis Letters Vol. 105, Nos. 3–4, December 2005 (© 2005)
DOI: 10.1007/s10562-005-8686-5

Comparison of $CuO/Ce_{0.8}Zr_{0.2}O_2$ and CuO/CeO_2 catalysts for low-temperature CO oxidation

Shu-Ping Wang[a], Xiu-Cheng Zheng[b], Xiao-Ying Wang[a], Shu-Rong Wang[a], Shou-Min Zhang[a], Li-Hua Yu[a], Wei-Ping Huang[a], and Shi-Hua Wu[a,]*

[a]*Department of Chemistry, Nankai University, Tianjin 300071, China*
[b]*Department of Chemistry, Zhengzhou University, Zhengzhou 450052, China*

Received 21 July 2005; accepted 6 September 2005

$CuO/Ce_{0.8}Zr_{0.2}O_2$ and CuO/CeO_2 catalysts were prepared via a impregnation method characterized by using FT-Raman, XRD, XPS and H_2-TPR technologies. The catalytic activity of the samples for low-temperature CO oxidation was investigated by means of a microreactor-GC system. The influence of the calcination temperature and different supports on the catalytic activity was studied.

KEY WORDS: $CuO/Ce_{0.8}Zr_{0.2}O_2$; CuO/CeO_2; CO oxidation.

1. Introduction

Carbon monoxide, emitted from many industrial processes and automobile exhausts, has been considered as a major air pollution. In order to control the toxic emission, catalytic oxidation is an efficient way. A number of catalysts have been studied in the past decades. Among them, precious metal catalysts have giving promising results because of their high catalytic activities for low-temperature CO oxidation [1–6]. However, the employment of noble metal catalysts is limited due to their scarce and high cost. Hence, it is important to find an alternative catalytic component to replace the noble metal and attentions have been given to base metal as catalysts, especially copper oxide [7–11].

Ceria, as known to all, is one of the major supports widely applied in the automotive three-way catalytic converter and has been widely investigated for the past few years. Among various functions of CeO_2, oxygen storage action is the most important one, which provided by the redox couple "Ce^{4+}/Ce^{3+}" making more oxygen available for the oxidation processes [12]. However, it is known that the pure CeO_2 has poor thermal stability. A loss in surface area also occurs due to the changes in pore structure and in crystallite growth. The structural modification and perfection of the CeO_2 lattice by doping with other rare earth or transition metal oxides may improve the stability of the surface area of ceria at high temperature [13]. Recently, there is much interest in a new generation of mixed oxide containing CeO_2 and ZrO_2. It has been reported that the addition of ZrO_2 to ceria can control the structure or the sites of ceria crystallite and form a Ce–Zr–O solid solution, which causes the improvements in the oxygen storage capacity (OSC), redox property and thermal resistance [1,14–18]. To the best of our knowledge, few literatures have been reported on the comparative study of $Ce_{0.8}Zr_{0.2}O_2$ solid solution and CeO_2 supported copper oxide as catalysts for low-temperature CO oxidation.

In our present work, we prepared $Ce_{0.8}Zr_{0.2}O_2$ solid solution employing a conventional co-precipitation starting from $ZrOCl_2 \cdot 8H_2O$ and $Ce(NO_3)_3 \cdot 6H_2O$ and $CuO/Ce_{0.8}Zr_{0.2}O_2$ catalysts using a impregnation method. For the purpose of comparison, CeO_2 and CuO/CeO_2 catalysts were also prepared via the similar method. The catalysts were characterized by means of XRD, FT-Raman, XPS and H_2-TPR. The catalytic activities of the catalysts were tested by using a microreactor-GC system.

2. Experimental

2.1. Catalyst preparation

Nanocrystalline $Ce_{0.8}Zr_{0.2}O_2$ mixed oxide was prepared by using a conventional co-precipitation. Of 2.42 g $ZrOCl_2 \cdot 8H_2O$ and 13.04 g $Ce(NO_3)_3 \cdot 6H_2O$ were dissolved into 160 mL distilled water under vigorous stirring, then 2 mol/L $NH_3 \cdot H_2O$ was added, drop by drop, into the above solution until the $pH = 9$. The transparent solution gradually changed into brown-gray color. The solution was centrifuged, and washed with deionized water and absolute ethanol until chloride ions cannot be detected using $AgNO_3$ solution, then the prepared precipitate was calcined at 600 °C in muffle furnace for 4 h.

The supported $CuO/Ce_{0.8}Zr_{0.2}O_2$ were prepared by the impregnation method using an aqueous solution of

---

* To whom correspondence should be addressed.
E-mail: wushh@nankai.edu.cn

$Cu(NO_3)_2 \cdot 3H_2O$ and $Ce_{0.8}Zr_{0.2}O_2$ prepared above. The prepared samples were dried at 800 °C for 12 h, then calcined at 400, 500, 600 and 800 °C for 4 h in the the muffle furnace, respectively. The CuO loading was 5 wt.%.

The CeO_2 support and CuO/CeO_2 catalysts were prepared in the similar manner as described above starting from $Ce(NO_3)_3 \cdot 6H_2O$ and $Cu(NO_3)_2 \cdot 3H_2O$, respectively. The CuO loading was also 5 wt.%.

2.2. Catalyst characterization

Fourier transform (FT) Raman spectra were recorded with a RTS 100/S FT-RAMAN spectrometer (BRUKER, Germany) with liquid N_2 detector, using the 1064-nm excitation line of Nd-YAG laser. The date was collected by keeping the power at 60 mW. The sample powders were pressed into small disc and then mounted on the analytic chamber.

X-ray powder diffraction (XRD) analyses were obtained from a D/MAX-2500 diffractometer using CuKα radiation (40 kV, 100 mA) and scanning in the region $2\theta = 15°–80°$. The average crystallite sizes were calculated from the peak width using the Scherrer's equation.

X-ray photoelectron spectra (XPS) were recorded on a PHI-1600 spectrometer (USA) equipped with a MgKα radiation for exciting photoelectrons. X-ray source was operated at an accelerating voltage of 15 kV and 250 W. The pressure in the ion-pumped analysis chamber was maintained at 8×10^{-10} Torr (1 Torr = 133.33 Pa) during data acquisition. All binding energies (BE) were referenced to the adventitious C1s line at 284.6 eV (1 eV = 1.602×10^{-19} J).

Temperature-programmed reduction (TPR) experiments were performed under the mixture of 5% H_2 in N_2 flowing (30 mL/min) over 0.1 g catalyst at a heating rate of 10 °C/min. Prior to TPR, the samples were treated in air at 200 °C for 30 min. The H_2 uptake amount during the reduction was measured by using a thermal conductivity detector (TCD).

2.3. Catalytic activity

The catalytic activity measurements of the catalysts were carried out in a fixed bed flow microreactor (7 mm i.d.) under atmospheric pressure using 0.05 g of catalyst powder doping with 2.00 g SiO_2. The airflow rate was 33.3 mL/min, and the CO gas flow rate was 0.5 mL/min. The reactant and product composition were analyzed on-line by a GC-508A gas chromatograph equipped with a thermal conductivity detector (TCD).

3. Results and discussion

3.1. Catalyst characterization

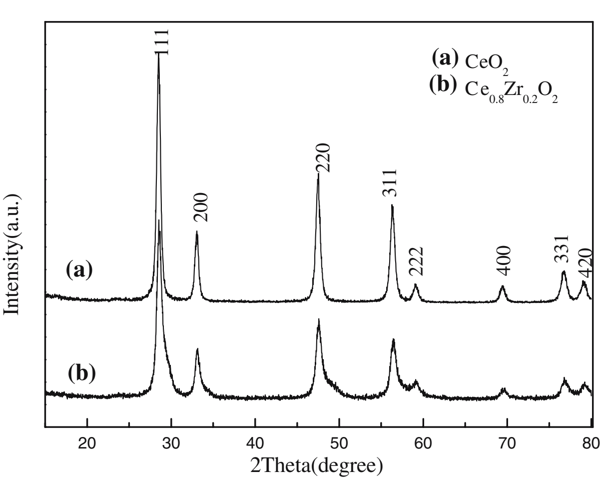

Figure 1. XRD patterns of CeO_2 and $Ce_{0.8}Zr_{0.2}O_2$ supports.

X-ray diffraction patterns of the prepared CeO_2 and $Ce_{0.8}Zr_{0.2}O_2$ supports are shown in figure 1. It was indicated the presence of a true cubic, fluorite structure typical of CeO_2 (indexed in the cubic Fm3m space group) for the CeO_2 particles. The structure of the prepared $Ce_{0.8}Zr_{0.2}O_2$ was consistent with that of the CeO_2, and there was no indication of the presence of other phases. The results indicated that the zirconia dopant is contained within the lattice and not as a separate phase. The lack of free ZrO_2 in the $Ce_{0.8}Zr_{0.2}O_2$ was also confirmed by Raman spectroscopy (figure 2).

The particle sizes of CeO_2 and $Ce_{0.8}Zr_{0.2}O_2$ were about 28.2 and 17.5 nm, which were showed in table 1. Due to the ionic radius of Zr^{4+} (0.72 Å) was smaller than that of Ce^{4+} (1.034 Å), the grain size of $Ce_{0.8}Zr_{0.2}O_2$ was smaller than CeO_2. This may also indicated that the zirconia dopant is contained within the lattice and Ce and Zr were highly homogeneously distributed. The different intensity of the two samples may originate from the different degree of porosity and crystallinity of CeO_2 and $Ce_{0.8}Zr_{0.2}O_2$.

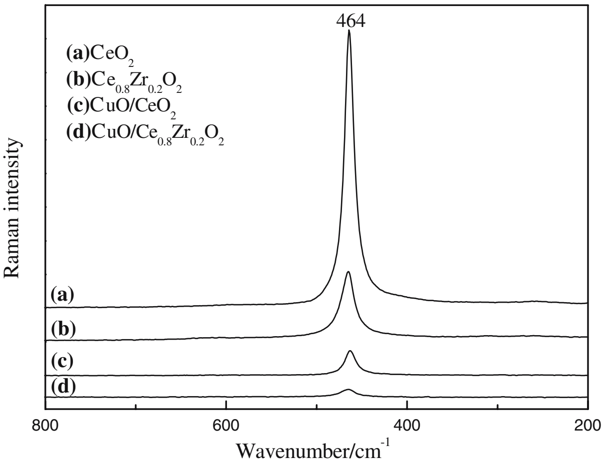

Figure 2. Raman spectra of CeO_2, $Ce_{0.8}Zr_{0.2}O_2$, CuO/CeO_2 and $CuO/Ce_{0.8}Zr_{0.2}O_2$ catalysts calcined at 500 °C.

Table 1
Supports particle size of the catalysts

Sample	Calcination temperature (°C)	Particle size (nm)
CeO_2	–	28.2
$Ce_{0.8}Zr_{0.2}O_2$	–	17.5
$CuO/Ce_{0.8}Zr_{0.2}O_2$	400	17.5
$CuO/Ce_{0.8}Zr_{0.2}O_2$	500	17.5
$CuO/Ce_{0.8}Zr_{0.2}O_2$	600	18.2
$CuO/Ce_{0.8}Zr_{0.2}O_2$	800	30.4
CuO/CeO_2	400	24.1
CuO/CeO_2	500	26.4
CuO/CeO_2	600	23.4
CuO/CeO_2	800	92.7

The Raman spectra of the CeO_2, $Ce_{0.8}Zr_{0.2}O_2$, CuO/CeO_2 and $CuO/Ce_{0.8}Zr_{0.2}O_2$ are shown in figure 2. It was found that there was only one strong adsorption peak centered at about 464 cm^{-1} for the CeO_2 and $Ce_{0.8}Zr_{0.2}O_2$ samples, which is typical of the F_{2g} Raman active mode of a fluorite structured material [19]. The results were in good agreement with the XRD analyses, which also indicated the presence of only the cubic, fluorite structure type. This also suggested the consistence in structure for CeO_2 and $Ce_{0.8}Zr_{0.2}O_2$. Furthermore, no obvious CuO peak appeared at about 298 cm^{-1} in the CuO/CeO_2 and $CuO/Ce_{0.8}Zr_{0.2}O_2$ catalysts curves, indicating that CuO was highly dispersed on the surface of the supports.

Figure 3 shows the XRD patterns of the $CuO/Ce_{0.8}Zr_{0.2}O_2$ catalysts calcined at different temperatures. It showed that no obvious peaks attributed to CuO crystal phase could be observed for the samples calcined at 400, 500 and 600 °C, which indicated that CuO is finely dispersed on $Ce_{0.8}Zr_{0.2}O_2$. However, when it was calcined at 800 °C, two CuO characteristic peaks appeared obviously. The $Ce_{0.8}Zr_{0.2}O_2$ average sizes in these catalysts were listed in table 1. It was noted that the supports had similar sizes when the calcination temperature was lower than 600 °C. While the particle size increased much larger in the catalyst calcined at 800 °C. It indicated that sample was sintered at high temperature and the bulk CuO had formed on the $Ce_{0.8}Zr_{0.2}O_2$ surface, which may be due to that the CuO dispersion degree was decreased with the sinter of the catalyst.

Figure 4 shows the XRD patterns of the CuO/CeO_2 catalysts calcined at different temperatures. Table 1 shows the average particle sizes of CeO_2 in these catalysts. It can be found that the catalysts calcined at 400, 500 and 600 °C had no obvious CuO diffraction peaks appeared. From table 1 we can see that the particle sizes of these samples were close to each other. But for the catalyst calcined at 800 °C, two obvious diffraction peaks of CuO could be observed and the particle size increased largely. Compared to $CuO/Ce_{0.8}Zr_{0.2}O_2$, the change of the support particle size in the CuO/CeO_2 catalyst calcined at 800 °C was much more obvious. This might because CuO/CeO_2 catalyst was sintered more seriously than $CuO/Ce_{0.8}Zr_{0.2}O_2$ catalyst and the dispersion of CuO on the support surface decreased obviously, which may influence catalytic activity greatly.

Figure 5 shows the XPS spectra of O 1s (1) and Cu 2p (2) binding energies of 5 wt.% CuO/CeO_2 and $CuO/Ce_{0.8}Zr_{0.2}O_2$ calcined at 500 °C for 4 h. It can be found that O 1s shows two main peaks, one at about 531.4 eV is attributed to the absorbed oxygen [20] and the other at 529.2 eV represents the lattice oxygen associated with metal oxides [21]. The peaks centered at 932.3 and 952.3 eV represent the Cu $2p_{3/2}$ and Cu $2p_{1/2}$, respectively. The Cu $2p_{3/2}$ values of these samples were lower than that of CuO, 933.6 eV [22]. We think that it may suggest the presence of reduced copper species in the catalysts, however, it was less convincing to distinguish between Cu_2O and Cu^0 and this needs further study.

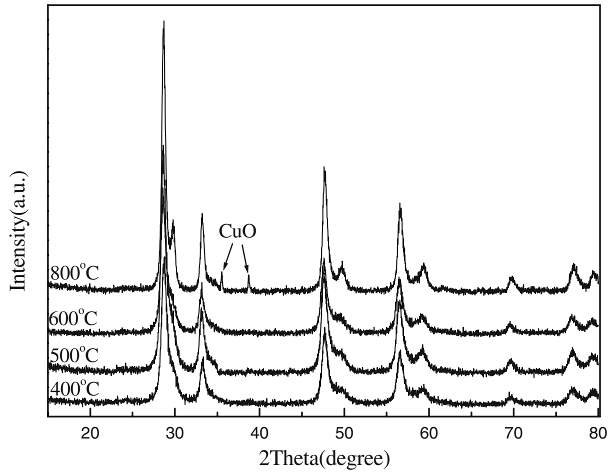

Figure 3. XRD patterns of $CuO/Ce_{0.8}Zr_{0.2}O_2$ catalysts calcined at different temperatures.

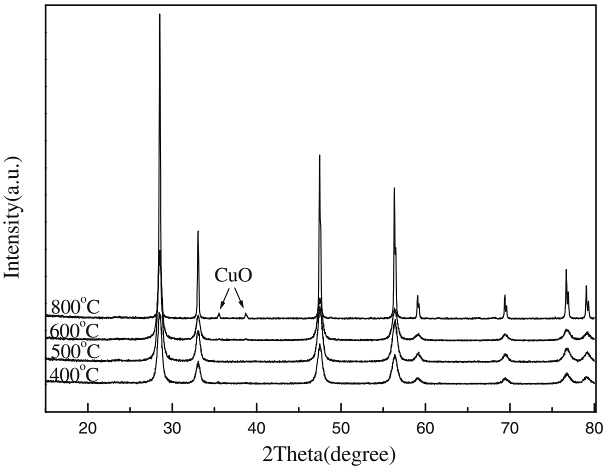

Figure 4. XRD patterns of CuO/CeO_2 catalysts calcined at different temperatures.

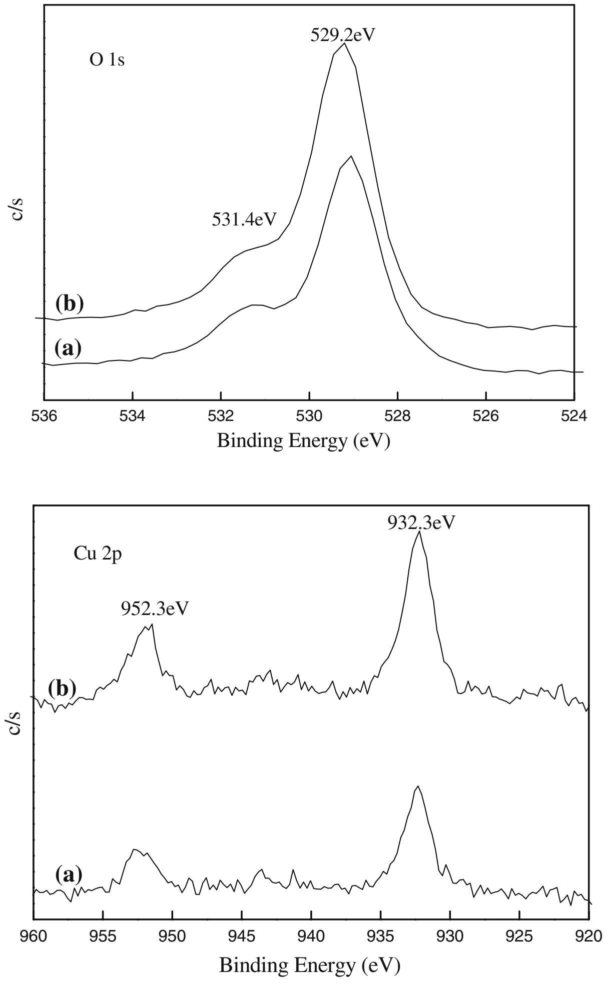

Figure 5. XPS patterns of O 1s (1) and Cu 2p (2) for (a) CuO/CeO_2, (b) $CuO/Ce_{0.8}Zr_{0.2}O_2$.

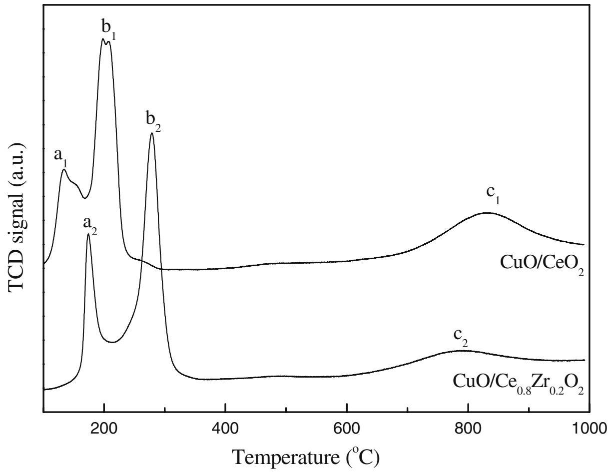

Figure 6. H_2-TPR profiles of $CuO/Ce_{0.8}Zr_{0.2}O_2$ and CuO/CeO_2 catalysts calcined at 500 °C.

In order to study the reduction ability of CuO supported on different supports, we did the H_2-TPR analyses. Figure 6 shows the typical H_2-TPR profiles of $CuO/Ce_{0.8}Zr_{0.2}O_2$ and CuO/CeO_2 catalysts calcined at 500 °C. For CuO/CeO_2, mainly two reduction peaks a_1 and b_1 were observed at about 132.3 and 201.3 °C. Meanwhile, there was another peak c_1 presented at about 830.3 °C due to the reduction of CeO_2 [23–25]. While there were only two low temperature reduction peaks a_2 and b_2 at about 172.1 and 278.5 °C for $CuO/Ce_{0.8}Zr_{0.2}O_2$, and peak c_2 can be observed at 777.4 °C due to the reduction of $Ce_{0.8}Zr_{0.2}O_2$ [23–25]. The result showed that the presence of zirconia decreased the reduction temperature from 830.3 to 777.4 °C, indicating the increase in reducibility of the support. On the other hand, at least two reduction peaks were observed in the catalysts, indicating the existence of different type of CuO species.

Several groups have investigated the TPR of CuO supported on CeO_2 and Ce–Zr–O solid oxide [26–28]. The reduction peaks of CuO in the range 120–170 °C and above 200 °C were observed. While for pure CuO this occurred above 250 °C, the reduction temperature decreased for CuO in these literatures and also in our present study. Meanwhile the similar results have been observed for CeO_2 and $Ce_{0.8}Zr_{0.2}O_2$. This may be due to the synergistic effects between CuO and the supports, which result in lower reduction temperature for both CuO and the supports. According to above analyses, we believed that the reduction peak a_1 for CuO/CeO_2 and the peak a_2 for $CuO/Ce_{0.8}Zr_{0.2}O_2$ were attributed to the reduction of highly dispersed CuO strongly interacting with support. While the peak b_1 for CuO/CeO_2 was attributed to the reduction of larger CuO species on the ceria surface weekly associated with the support, and the peak b_2 for $CuO/Ce_{0.8}Zr_{0.2}O_2$ (about 278.5 °C) probably arose from the reduction of bulk CuO. The TPR analyses showed that bulk CuO particles did not appear in the present CuO/CeO_2 sample and the CuO dispersion degree on the CeO_2 surface support was higher than that on the $Ce_{0.8}Zr_{0.2}O_2$ support. Furthermore, the reduction temperature of the CuO supported on CeO_2 was lower than that on $Ce_{0.8}Zr_{0.2}O_2$. The results may make the CuO/CeO_2 catalysts have higher catalytic activity than $CuO/Ce_{0.8}Zr_{0.2}O_2$ catalysts under the same reaction condition.

3.2. *Catalytic activity for CO oxidation*

Figure 7 shows the catalytic activity for CO oxidation of $CuO/Ce_{0.8}Zr_{0.2}O_2$ catalysts calcined at different temperatures. It can be observed that the CO conversion increased with the increasing reaction temperature for all the catalysts. Furthermore, the catalytic activity of the $CuO/Ce_{0.8}Zr_{0.2}O_2$ catalysts increased with the calcination temperature and the catalyst calcined at 600 °C exhibited the highest catalytic activity. However, when the catalyst calcined at 800 °C the catalytic activity decreased, which may be due to the sinter of CuO/

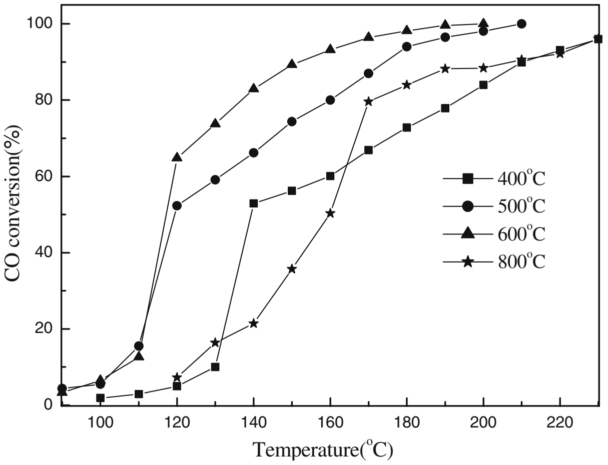

Figure 7. Catalytic activity for CO oxidation of $CuO/Ce_{0.8}Zr_{0.2}O_2$ catalysts calcined at different temperatures.

$Ce_{0.8}Zr_{0.2}O_2$ catalyst at high temperature. The "light-off" temperature for 100% CO conversion over $CuO/Ce_{0.8}Zr_{0.2}O_2$ calcined at 500 and 600 °C was about 210 and 200 °C, respectively. But the maximal CO conversion date on the catalysts calcined at 400 and 800 °C were both about 96% in the present case.

Figure 8 presents the catalytic activity for CO oxidation of CuO/CeO_2 catalysts calcined at different temperatures. It was noted that the catalytic activity of CuO/CeO_2 enhanced with increasing the calcination temperature from 400 to 500 °C, but it decreased above 500 °C. The "light-off" temperature for 100% CO conversion over CuO/CeO_2 calcined at 400, 500 and 600 °C were about 180, 150 and 180 °C, respectively. When the calcination temperature increased to 800 °C, the catalytic activity obviously fell down to below 20% in the present case. This is due to the fact that CuO/CeO_2 was sintered more seriously than $CuO/Ce_{0.8}Zr_{0.2}O_2$ catalysts at high temperatures. That is to say, the $CuO/Ce_{0.8}Zr_{0.2}O_2$ had higher thermal resistance than the CuO/CeO_2 catalysts. However, the reason needs further study.

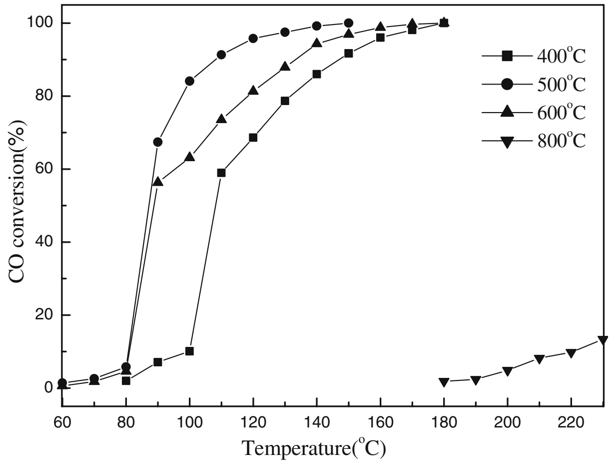

Figure 8. Catalytic activity for CO oxidation of CuO/CeO_2 catalysts calcined at different temperatures.

From figures 7 and 8, it can be seen that the CuO/CeO_2 exhibited higher catalytic activity than $CuO/Ce_{0.8}Zr_{0.2}O_2$ when the calcinations temperature was lower than 600 °C. But for the catalysts calcined at 800 °C, the result was just the opposite. Luo et al. [29] suggested that dispersed CuO was responsible for the high catalytic activity for low-temperature CO oxidation. In the present case, the temperature for 100% CO conversion over CuO/CeO_2 and $CuO/Ce_{0.8}Zr_{0.2}O_2$ calcined at 500 °C was 150 and 210 °C, respectively. According to the above TPR analyses, the CuO/CeO_2 catalyst calcined at 500 °C has higher CuO dispersion degree and lower reduction temperature compared with the $CuO/Ce_{0.8}Zr_{0.2}O_2$ catalyst, which may be the reason for the difference of the catalytic activity.

4. Conclusions

In this study, only cubic phase were observed for CeO_2, $Ce_{0.8}Zr_{0.2}O_2$ and also for the supports in the CuO/CeO_2 and $CuO/Ce_{0.8}Zr_{0.2}O_2$ catalysts by XRD and FT-Raman analyses. Combing the results of XRD, FT-Raman, XPS, H_2-TPR and catalytic activity measurements, we believed that the well-dispersed CuO is responsible for low-temperature CO oxidation. The CuO/CeO_2 exhibited higher catalytic activity than $CuO/Ce_{0.8}Zr_{0.2}O_2$ catalysts when the calcination temperature was lower than 600 °C. However, the result was just the opposite when the catalysts calcined at 800 °C. This indicated that $CuO/Ce_{0.8}Zr_{0.2}O_2$ had better thermal resistance than CuO/CeO_2 catalysts and this needs further study.

Acknowledgments

This work was supported by the National Natural Science Foundation of China (No. 20271028) and Tianjin Natural Science Foundation (No. 033602511).

References

[1] J.A. Wang, L.F. Chen, M.A. Valenzuela, A. Montoya, J. Salmones and P.D. Angel, Appl. Surf. Sci. 230 (2004) 34.

[2] A. Martorana, G. Deganello, A. Longo, A. Prestianni, L. Liotta, A. Macaluso, G. Pantaleo, A. Balerna and S. Mobilio, J. Solid State Chem. 177 (2004) 1268.

[3] E. Bekyarova, P. Fornasiero, J. Kašpar and M. Graziani, Catal. Today 45 (1998) 179.

[4] P. Fornasiero, J. Kašpar, V. Sergo and M. Graziani, J. Catal. 182 (1999) 56.

[5] Q. Xu, K.C.C. Kharas and A.K. Datye, Catal. Lett. 85 (2003) 229.

[6] M.-F. Luo, Y.-Y. Hou, X.-X. Yuan and X.-M. Zheng, Catal. Lett. 50 (1998) 205.
[7] B. Wen and M.-Y. He, Appl. Catal. B 37 (2002) 75.
[8] H.-Y. Zhu, M.-M. shen, Y. Kong, J.-M. Hong, Y.-H. Hu, T.-D. Liu, L. Dong, Y. Chen, C. Jian and Z. Liu, J. Mol. Catal. A 219 (2004) 155.
[9] A. George, I. Theophilos, M. Haralambos, B. Jurka and H. Stanko, Catal. Lett. 73 (2001) 33.
[10] L. Dong, Y. Hu, M. Shen, T. Jin, J. Wang, W. Ding and Y. Chen, Chem. Mater. 13 (2001) 4227.
[11] X.-C. Zheng, S.-H. Wu, S.-P. Wang, S.-R. Wang, S.-M. Zhang and W.-P. Huang, Appl. Catal. A 283 (2005) 217.
[12] K. Min, M.-W. Song and C.H. Lee, Appl. Catal. A 251 (2003) 143.
[13] A. Trovarelli, C. De Leitenburg, M. Boaro and R. Dolcetti, Catal. Today 50 (1999) 353.
[14] X.-Y. Liu, S.-D. Wang, Z.-S. Yuan, J. Zhou, N. Liu, C.-X. Zhang and G.-Z. Fu, Chin. J. Catal. 25 (2004) 91.
[15] R. Si, Y.-W. Zhang, C.-X. Xiao, S.-J. Li, B.-X. Lin, Y. Kou and C.-H. Yan, Phys. Chem. Chem. Phys. 6 (2004) 1056.
[16] M. Daturi, E. Finocchio, C. Biinet, J.C. Lavalley, F. Fally, V. Perrichon, H. Vidal, N. Hickey and J. Kaspar, J. Phys. Chem. B 104 (2000) 9186.
[17] T. Masui, T. Ozaki, K. Machida and G. Adachi, J. Alloys. Compounds 303 (2000) 49.
[18] E.S. Putna, T. Bunluesin, X.L. Fan, R.J. Gorte, J.M. Vohs, R.E. Lakis and T. Egami, Catal. Today 50 (1999) 343.
[19] J.E. Spanier, R.D. Robinson, F. Zheng, S.W. Chan and I.P. Herman, Phys. Rev. B 64 (2001) 245407.
[20] X.-C. Zheng, S.-P. Wang, S.-M. Zhang, S.-R. Wang, W.-P. Huang and S.-H. Wu, React. Kinet. Catal. Lett. 84 (2005) 29.
[21] A.E. Nelson and K.H. Schulz, Appl. Surf. Sci. 210 (2003) 206.
[22] G. Avgouropoulos and T. Ioannides, Appl. Catal. A 244 (2003) 155.
[23] K. Otsuka, W. Ye and M. Nakamura, Appl. Catal. A 183 (1999) 317.
[24] J. Kaspar, P. Fornasiero and M. Graziani, Catal. Today 50 (1999) 285.
[25] F. Fally, V. Perrichon, H. Vidal, J. Kaspar, G. Blanco, J.M. Pintado, S. Bernal, G. Colon, M. Daturi and J.C. Lavalley, Catal. Today 59 (2000) 373.
[26] W. Liu and M. Flytzani-Stephanopoulos, Chem. Eng. J 64 (1996) 283.
[27] L. Kundakovic and M. Flytzani-Stephanopoulos, Appl. Catal. A 171 (1998) 13.
[28] P. Ratnasamy, D. Srinivas, C.V.V. Satyanarayana, P. Manikandan, R.S.S. Kumaran, M. Sachin and V.N. Shetti, J. Catal. 221 (2004) 455.
[29] M.-F. Luo, Y.-Y. Hou, X.-X. Yuan and X.-M. Zheng, Catal. Lett. 50 (1998) 205.